

CrystEngComm

Accepted Manuscript



This is an *Accepted Manuscript*, which has been through the Royal Society of Chemistry peer review process and has been accepted for publication.

Accepted Manuscripts are published online shortly after acceptance, before technical editing, formatting and proof reading. Using this free service, authors can make their results available to the community, in citable form, before we publish the edited article. We will replace this *Accepted Manuscript* with the edited and formatted *Advance Article* as soon as it is available.

You can find more information about *Accepted Manuscripts* in the [Information for Authors](#).

Please note that technical editing may introduce minor changes to the text and/or graphics, which may alter content. The journal's standard [Terms & Conditions](#) and the [Ethical guidelines](#) still apply. In no event shall the Royal Society of Chemistry be held responsible for any errors or omissions in this *Accepted Manuscript* or any consequences arising from the use of any information it contains.



Crystal growth and structural remarks in malonate-based lanthanide coordination polymers

Fernando S. Delgado,^a Pablo Lorenzo-Luis,^b Jorge Pasán,^a Laura Cañadillas-Delgado,^c Oscar Fabelo,^d María Hernández-Molina,^e Antonio D. Lozano-Gorrín,^a Francesc Lloret,^f Miguel Julve^f and Catalina Ruiz-Pérez^{a,*}

Received 00th January 20xx,
Accepted 00th January 20xx

DOI: 10.1039/x0xx00000x

www.rsc.org/

The synthesis, structural characterization and thermal study of the new coordination polymers (CPs) of formula $[\text{Ln}_2(\text{mal})_3(\text{H}_2\text{O})_5] \cdot 2\text{H}_2\text{O}$ [$\text{Ln} = \text{Ho}$ (**1-2H₂O**), Tb (**1a**), Dy (**1b**), Er (**1c**) and Yb (**1d**); mal = malonate], $[\text{Ln}_2(\text{mal})_3(\text{H}_2\text{O})_6]$ [$\text{Ln} = \text{Sm}$ (**2**) and Ce (**2a**)], $[\text{Ce}_2(\text{mal})_3(\text{H}_2\text{O})_6] \cdot 2\text{H}_2\text{O}$ (**3-2H₂O**) and $[\text{Ce}_2(\text{mal})_3(\text{H}_2\text{O})_3] \cdot 2\text{H}_2\text{O}$ (**4-2H₂O**) are presented. Complexes (**1-4**) have been also characterized by single crystal X-ray diffraction. The structure of **2** was previously reported (Elsegood, M. R. J.; Husain, S. *Private Communication* **2014**) and it is very close to that of **3**. In the light of these results and those previously reported in the literature for the malonate-containing lanthanide(III) complexes, a detailed overview on the crystal structures and topologies of these systems is provided herein covering CPs in one, two and three dimensions, as well as the molecular architectures assembled by hydrogen-bonding from low-dimensional entities to higher-dimensional supramolecular architectures.

1. Introduction

The design and synthesis of novel polymeric metal-organic complexes have attracted a great interest because of the growing realization of their potential use in magnetism, zeolite-like catalysis, gas storage, ion exchange, molecular recognition, optical and conducting devices, etc.¹

In this respect, considerable progress has been made on the theoretical prediction and network-based approaches to control the topology and geometries of the networks envisaging the production of functional materials.² Therefore, impressive research efforts are devoted to build novel coordination polymers (CPs) by using versatile organic ligands and metal ions.³ There has been an upsurge in the use of rare-earth elements as functional metal centres, due to the richness of their coordination chemistry, their special chemical characteristics arising from the presence of 4f electrons and their ability to form isostructural complexes.⁴ It is

well known that rare earth cations have a high affinity for hard donor atoms (ligands containing oxygen or hybrid oxygen-nitrogen atoms, for instance) and in particular, multicarboxylate ligands which are usually employed to build lanthanide coordination polymers.⁵ The use of flexible multicarboxylate ligands as connectors of the metal ions is very attractive because both the flexibility and conformational degrees of freedom of these ligands offer many possibilities for the construction of coordination frameworks with unique structures and useful properties. Recent studies show that the flexibility of the molecular backbones, their conformational preferences, the metal ions employed and their counter ions, all exert a strong influence on the polymeric structures obtained.⁶

The dicarboxylate ligands which are commonly used as ligands in the preparation of CPs with lanthanide ions range from relatively rigid species, such as benzene or naphthalene derivatives, to more flexible ones with alkyl chains between the peripheral carboxylate groups. The use of flexible ligands provides a significant contrast between the structures depending on the length of the alkyl chain, with polymers known that contain the $[\text{O}_2\text{C}-(\text{CH}_2)_n-\text{CO}_2]^{2-}$ linkers [$n = 1$ (malonate), 2 (succinate), 3 (glutarate) or 4 (adipate)], compared to other straight-chain anions such as fumarate or tartrate. However, the ability of the carboxylate group to adopt both chelating and bridging coordination modes means that the ligand cannot be often treated as a simple linear connector (like 4,4'-bipyridine) and the coordination networks are correspondingly more complex.

^aLaboratorio de Rayos X y Materiales Moleculares (MATMOL), Departamento de Física, Facultad de Ciencias (Sección Física), Universidad de La Laguna, Avda. Astrofísico Francisco Sánchez s/n, E-38204 La Laguna, Tenerife, Spain. E-mail: caruiz@ull.ull.es

^bDepartamento de Química, Facultad de Ciencias (Sección Química), Universidad de La Laguna, Avda. Astrofísico Francisco Sánchez s/n, E-38204 La Laguna, Tenerife, Spain.

^cCentro Universitario de la Defensa de Zaragoza, Ctra. Huesca s/n, 50090, Zaragoza, Spain

^dInstitut Laue Langevin, Diffraction Group, 71 Rue des Martyrs, 38008, Grenoble, France.

^eDepartamento de Ingeniería, Escuela Superior de Ingeniería, Universidad de La Laguna, Avda. Astrofísico Francisco Sánchez s/n, E-38204 La Laguna, Tenerife, Spain.

^fInstituto de Ciencia Molecular (ICMol), Universitat de València, C/ Catedrático José Beltrán 2, 46980 Paterna, València, Spain.

†Electronic Supplementary Information (ESI) available (pdf format) For ESI and crystallographic data in CIF or other electronic format see DOI: 10.1039/x0xx00000x

More flexible alkyl-based dicarboxylate as ligands adopt a variety of different conformations although the general trend of clusters or chains in their lanthanide complexes, as with the benzoate derivatives, is common to all. In general, aliphatic carboxylates exhibit the following features when considering their complexing ability: (i) mono- and bidentate coordination modes; (ii) *syn-syn*, *anti-anti* or *syn-anti* bridging conformations; (iii) tri-coordinated oxygen-atom connectivity; (iv) pillaring of the metal-oxygen layers or networks; (v) and generation of secondary building units (SBUs) by acting as capping agents through their carboxylate moieties.

The malonate ligand (dianion of the propanedioic acid, H₂mal) is one of the best exponents of the ability of flexible dicarboxylate ligands to build CPs. This ligand which has a methylene group between the two carboxylates is the shortest alkyldicarboxylate derivative. The methylene group is at the origin of its flexibility and great versatility as ligand. The malonate group can adopt different coordination modes in its complex formation (see **Scheme 1**) including the chelation to the metal ion to form a six-membered chelate ring (**Scheme 1b**).⁷ In contrast with the predictable crystal structures rationally designed with the more rigid oxalate dianion, the complex formation with the malonate ligand often gives unexpected results, new coordination modes and unpredictable behaviour which are the starting point for new polymers with new properties. Malonate-containing rare earth cations have been reported to undergo a temperature-dependent phase transition⁷ⁱ and even ferromagnetic coupling between gadolinium(III) ions through the double oxo(carboxylate) bridge.^{7k}

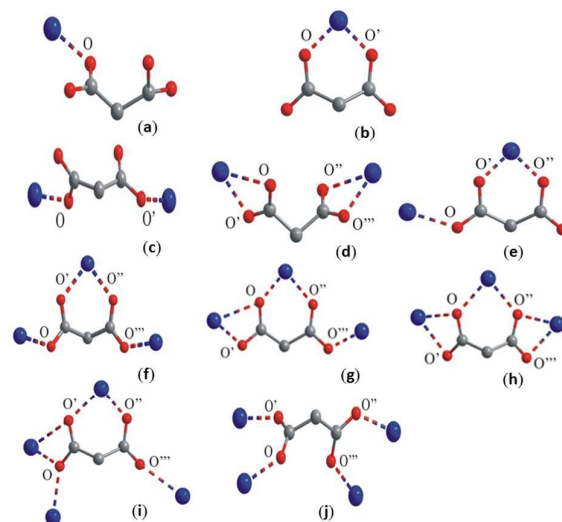
From a synthetic point of view, the variety of coordination modes of the malonate group represents a challenge. Its flexibility as a ligand does not allow the formation of a specific pattern in the coordination which can be repeated synthesis after synthesis. Moreover, subtle modifications in the synthetic procedure could afford different crystal structures. Therefore, studies of the new complexes of lanthanide ions with malonic acid are important from both fundamental and applied viewpoints.⁸⁻¹⁰

Having in mind the above considerations, our research has focused on the construction of novel coordination frameworks by using malonic acid as ligand towards rare earth cations, resulting in several series of lanthanide coordination polymers. Herein we first present the synthesis and X-ray structure of the malonate-containing lanthanide CPs of formula [Ln₂(mal)₃(H₂O)₅]-2H₂O [Ln = Ho (**1**), Tb (**1a**), Dy (**1b**), Er (**1c**) and Yb (**1d**)], [Ln₂(mal)₃(H₂O)₆] [Ln = Sm (**2**) and Ce (**2a**)], [Ce₂(mal)₃(H₂O)₆]-2H₂O (**3**) and [Ce₂(mal)₃(H₂O)₃]-2H₂O (**4**) together with their thermal study. Finally, these results are integrated in a thorough overview of the preparative routes and structural types of the homometallic malonate-containing rare-earth elements.

2. Experimental

2.1 Materials

Malonic acid, sodium metasilicate nonahydrate, sodium carbonate and a series of lanthanide(III) nitrate salts [Ln(NO₃)₃·6H₂O with Ln = Ce, Sm, Tb, Dy, Ho, Er and Yb] were purchased from commercial sources and used as received. Elemental analysis (C, H) were carried out on an EA 1108 CHNSO microanalytical instrument.



Scheme 1. Coordination modes of the malonate ligand: (a) κO ; (b) $\kappa^2 O, O$; (c) $\mu-\kappa O:\kappa O$; (d) $\mu-\kappa^2 O, O:\kappa^2 O'', O''$; (e) $\mu-\kappa O:\kappa^2 O', O''$; (f) $\mu_3-\kappa O:\kappa^2 O'; O'': \kappa O''$; (g) $\mu_3-\kappa^2 O:\kappa O': \kappa O''$; (h) $\mu_3-\kappa^2 O:\kappa O': \kappa^2 O'': \kappa O''$; (i) $\mu_4-\kappa^2 O:\kappa^2 O': \kappa O'': \kappa O''$ and (j) $\mu_4-\kappa O:\kappa O': \kappa O'': \kappa O''$.

2.2 Synthetic procedures

X-ray quality single crystals of the CPs of formula [Ho₂(mal)₃(H₂O)₅]-2H₂O (**1·H₂O**), [Ln₂(mal)₃(H₂O)₅]-2H₂O [Ln = Tb (**1a**), Dy (**1b**), Er (**1c**) and Yb (**1d**)], [Sm₂(mal)₃(H₂O)₆] (**2**), [Ce₂(mal)₃(H₂O)₆] (**2a**), [Ce₂(mal)₃(H₂O)₆]-2H₂O (**3·2H₂O**) and [Ce₂(mal)₃(H₂O)₃]-2H₂O (**4·2H₂O**) were obtained by following a similar method and then, only the preparation of the first compound is described in detail hereunder.

[Ho₂(mal)₃(H₂O)₅]-2H₂O (1·2H₂O**).** The synthesis of the holmium(III)-malonate was carried out by the reaction between malonic acid and holmium(III) nitrate in a sodium metasilicate gel. The silica gel was prepared by hydrolysis and polycondensation of sodium metasilicate nonahydrate in aqueous solution under acidic conditions.¹¹ The process involved primary mixing of proper amounts of 1 M Na₂SiO₃·9H₂O and 2 M malonic acid, to adjust the pH value of the mixed solutions to ca. 4.5. The mixture was introduced into test tubes and allowed to set for 24 hours at room temperature. An aqueous solution of 0.5 M holmium(III) nitrate was then added on the top of the gel dropwise, without disturbing the surface of the gel, and the tubes were covered with parafilm and stored at 30 °C. Colourless crystals of **1·2H₂O** suitable for X-ray analysis were grown after three weeks. They were removed from the gel, washed with water and dried at room temperature. Yield ca. 80%. Anal. calcd (found) % for C₉H₂₀Ho₂O₁₉ (**1·2H₂O**): C, 14.19 (14.08); H, 2.63 (2.59).

[Ln₂(mal)₃(H₂O)₅]-2H₂O with Ln = Tb (1a), Dy (1b), Er (1c) and Yb (1d). A mixture of malonic acid (1 mmol, 0.158 g) and sodium carbonate (1 mmol, 0.106 g) was dissolved in water (20 mL). An aqueous solution (10 mL) of the corresponding lanthanide(III) nitrate (0.66 mmol) was poured into the previous one under stirring. After 30 minutes, a white solid appeared which was filtered, washed with water and dried. Yield of **1a-d** greater than 90%. Anal. calcd (found) % for C₉H₂₀Tb₂O₁₉ (**1a**): C, 14.41 (14.34); H, 2.67(2.55). Anal. calcd (found) % for C₉H₂₀Dy₂O₁₉ (**1b**): C, 14.28(14.20); H, 2.64(2.57). Anal. Calcd (found) % for C₉H₂₀Er₂O₁₉ (**1c**): C, 14.10(14.01); H, 2.6(2.52). Anal. calcd(found) % for C₉H₂₀Yb₂O₁₉ (**1d**): C, 13.89(13.80); H, 2.57(2.49).

[Sm₂(mal)₃(H₂O)₆] (2). The preparation of **2** is performed by following the same procedure used for **1-2H₂O**. X-ray quality colourless needles of **2** appeared within three weeks. They were removed from the gel, washed and dried at room temperature. Yield 90%. Anal. calcd (found) % for C₉H₁₈Sm₂O₁₈ (**2**): C, 15.11(14.88); H, 2.52(2.23).

[Ce₂(mal)₃(H₂O)₆] (2a). The synthesis of **2a** follows the same procedure used for **1a-1d**. Yield greater than 90%. Anal. calcd (found) % for C₉H₁₈Ce₂O₁₈ (**2a**): C, 15.55(15.10); H, 2.59(2.26).

[Ce₂(mal)₃(H₂O)₆]-2H₂O (3-2H₂O) and [Ce₂(mal)₃(H₂O)₃]-2H₂O (4-2H₂O). These compounds were synthesized by using a procedure similar to that used for **1-H₂O**. Colourless prisms of **3-2H₂O** suitable for X-ray analysis appeared within two weeks in the upper part of the gel, afterwards colourless prisms of **4-2H₂O** appeared in the lower part. They were carefully removed from the gel, washed with water and air dried at room temperature. Overall yield: 73%. Anal. calcd. (found) % for C₉H₂₂Ce₂O₂₀ (**3-2H₂O**): C, 14.80(14.72); H, 3.01(2.91). Anal. calcd. (found) % for C₉H₁₆Ce₂O₁₇ (**4-2H₂O**): C, 15.98(15.88); H, 2.37(2.29).

2.3 Thermogravimetric analysis (TGA) and DSC measurements

Thermogravimetric (TG/DTA) and differential scanning calorimetry (DSC) studies were carried out on a PerkinElmer instrument (mod. Pyris Diamond) under a dinitrogen atmosphere (flow rate: 80 cm³ min⁻¹) from 25 to 350 °C. The samples (ca. 10 mg) were heated in an aluminum crucible (45 mL) at a rate of 5 °C min⁻¹. The TG curves were analyzed as mass loss (%) as a function of the temperature. The endo and exothermal processes were also identified by differential scanning calorimetry (DSC).

2.4 X-ray single-crystal diffraction

Single crystals of **1-4** were mounted on a Bruker-Nonius KappaCCD diffractometer. Orientation matrix and lattice parameters were obtained by least-squares refinement of the reflections obtained by a θ - ω scan (Dirax/lsq method). Diffraction data were collected at 293(2) K for **1-3** and at 173(2) K for **4**, using graphite-monochromated Mo-K α radiation ($\lambda = 0.71073$ Å). Data collection and data reduction were done with the COLLECT¹² and EVALCCD¹³ programs. Empirical absorption corrections were carried out by using SADABS¹⁴ for all compounds. All calculations for data reduction, structure solution, and refinement were done by standard procedures (WINGX).¹⁵ The structure was solved by direct methods and refined with full-matrix least-squares technique on F^2 using the SHELXS-97 and SHELXL-97 programs.¹⁶ The hydrogen atoms of the malonate ligand were set in calculated positions for compounds **1**, **3** and **4** whereas they were found from difference Fourier maps in the case of **2**. The hydrogen atoms for all compounds were refined with isotropic temperature factors. The final geometrical calculations and the graphical manipulations were carried out with PARST97¹⁷ and DIAMOND¹⁸ programs, respectively. A summary of the crystallographic data and refinement conditions is given in Table 1. Selected bond distances and intermolecular interactions for **1-4** are shown in Tables S1-S4, ESI†. CCDC-294297, CCDC-294298, CCDC-294299, CCDC-1475076 contains the supplementary crystallographic data for **1-4**, respectively.

2.5 X-ray powder diffraction (XPRD)

The identity of the bulk material obtained from precipitation (case of compounds **1a-1d** and **2a**) was verified by comparison of their XRPD patterns with the simulated ones of the published Ln-malonate complexes. The XRPD patterns were collected with a PANalytical X'Pert Pro diffractometer equipped with an X'Celerator detector and a primary monochromator, using Cu-K α radiation, in the angular range $5 \leq 2\theta \leq 80^\circ$, by step scanning in equivalent increments of 0.02°. The data were fitted, on the basis of the single crystal structure determination, by using the Rietveld method¹⁹ through the Fullprof program.²⁰ The peak shape was described through a pseudo-Voigt function whereas a polynomial function with five refinable coefficients was used for the background.

Table 1. Crystal data and details of the structure determination for compounds **1-4**.

Compound	1·2H₂O	2	3·2H₂O	4·2H₂O
<i>T</i> , K	293(2)	293(2)	293(2)	173(2)
Formula	C ₉ H ₂₀ Ho ₂ O ₁₉	C ₉ H ₁₈ Sm ₂ O ₁₈	C ₉ H ₂₂ Ce ₂ O ₂₀	C ₉ H ₂₂ Ce ₂ O ₁₇
<i>M</i>	762.11	714.93	730.51	676.46
Crystal system	orthorhombic	monoclinic	orthorhombic	monoclinic
Space group	<i>Pnma</i>	<i>C2/c</i>	<i>Pbcn</i>	<i>P2₁</i>
<i>a</i> , Å	12.0794(12)	17.150(2)	11.3106(7)	7.6281(8)
<i>b</i> , Å	8.0555(9)	12.284(2)	12.6698(12)	12.8621(13)
<i>c</i> , Å	20.207(3)	11.144(2)	14.7397(15)	8.8824(11)
β , deg		127.549(13)		101.279(8)
<i>V</i> , Å ³	1966.3 (4)	1861.3(5)	2112.2(3)	854.65(16)
<i>Z</i>	4	4	4	2
ρ_{calc} (Mg m ⁻³)	2.574	2.551	2.297	2.629
<i>F</i> (000)	1440	1360	1408	644
λ (Mo-K α) Å	0.71073	0.71073	0.71073	0.71073
μ (Mo-K α) (mm ⁻¹)	8.083	6.339	4.349	5.351
Number parameters/restraints	151/0	144/0	142/0	254/1
Goodness of fit (<i>S</i>)	1.227	1.160	1.109	1.078
<i>R</i> 1, <i>I</i> > 2 σ (<i>I</i>) (all)	0.0333 (0.0376)	0.0321 (0.0430)	0.0415 (0.0624)	0.0297 (0.0337)
<i>wR</i> 2, <i>I</i> > 2 σ (<i>I</i>) (all)	0.0814 (0.0831)	0.0797 (0.0897)	0.0926 (0.1024)	0.0653 (0.0667)
Max/min electron density (e/Å ³)	1.363 / -1.606	1.147 / -2.334	1.400 / -2.095	1.538 / -0.934
Measured reflections (<i>R</i> _{int})	50047 (0.0711)	8232(0.0525)	13060(0.0962)	13633 (0.0515)
Independent reflections [<i>I</i> > 2 σ (<i>I</i>)]	2418 (2247)	2708 (2366)	3051 (2324)	3879
Flack parameter				0.06(3)

3 Results and discussion

3.1 Crystal structures

The three new complexes **1·2H₂O**, **3·2H₂O** and **4·2H₂O** are isostructural with previously reported complexes.⁷ The structure of **2** has been previously reported as a private communication^{7t} and it has been included herein for comparative purposes.

[Ho₂(mal)₃(H₂O)₅]·2H₂O (1·2H₂O). Single-crystal X-ray analysis reveals that complex **1** consists of malonate-bridged diaqua- and triaquaholmium(III) units that lead to two-dimensional arrays stacked along the crystallographic *c* axis (Fig. 1). Each Ho(III) cation within these layers is linked to other four metal centres through the bridging modes of Scheme 1f and 1g, forming a topological 6³-*hcb* Shubnikov hexagonal plane net. The layers are interlinked by means of hydrogen bonds involving one crystallization water molecule affording a supramolecular three-dimensional structure (Fig. 2 and Table S1, ESI†).

Two crystallographically independent holmium(III) cations [Ho(1) and Ho(2)] occur in **1·2H₂O** (Fig. 3). They lie on a mirror plane and exhibit nine- [Ho(1)] and eight- [Ho(2)] coordination. Six oxygen atoms from three different malonate groups [Ho(1)-O(mal) bond distances being equal to 2.307(4), 2.363(4) and 2.843(4) Å] and

three water molecules [values of the Ho(1)-O(w) bond lengths of 2.366(6), 2.343(6) and 2.346(6) Å] build a distorted tricapped trigonal prism around the Ho(1) atom, whereas Ho(2) is surrounded by six oxygen atoms from four different malonate groups [Ho(2)-O(mal) bond distances being 2.313(4), 2.318(4) and 2.377(4) Å] and two water molecules [Ho(2)-O(w) = 2.366(6) and 2.404(6) Å] forming a distorted square antiprism. Similar geometries have been observed in the isostructural related compounds [Eu₂(mal)₃(H₂O)₅]·3H₂O^{7c} and [Gd₂(mal)₃(H₂O)₅]·2H₂O.^{7m}

Two aspects concerning the holmium environment deserves to be noted: (i) The longer value of the Ho(1)-O(1) bond in **1·2H₂O** which is due to the geometrical constraints associated to the four-membered chelating ring subtended by the O(2)C(1)O(1) carboxylate group at the Ho(1) atom; (ii) the mean value of the Ho-O(w) bond distance [2.358(6) Å] which is longer than the one of the Ho-O(mal) bonds [2.336(4) Å]. All coordinated water molecules in **1·2H₂O** lie on a mirror plane.

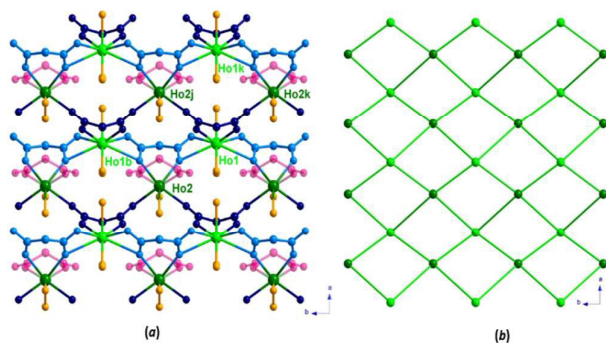


Fig. 1. Perspective (a) and schematic (b) views along the crystallographic *c*-axis of a fragment of the malonate-bridged holmium(III) layers in CP **1·2H₂O**.

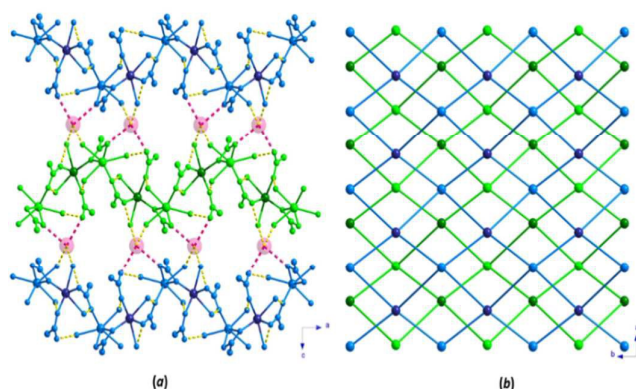


Fig. 2. Perspective (a) and schematic (b) views along the crystallographic *b*- and *c*-axis of the stacking of the holmium(III) malonate layers in **1·2H₂O**.

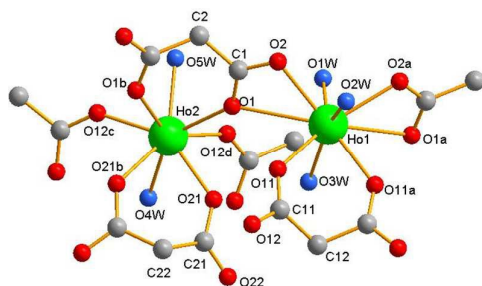


Fig. 3. A view of the holmium environments in **1·2H₂O** showing the atom numbering. Symmetry code: a: $x, -y-1/2, z$; b: $x, -y+1/2, z$; c: $x-1/2, -y+1/2, -z-1/2$; d: $+x-1/2, y, -z-1/2$.

Three crystallographically independent malonate groups are present in **1·2H₂O** (Fig. 4): L1 [C(1)C(2)C(1b)], L2 [C(11)-C(12)-C(11a)] and L3 [C(21)-C(22)-C(21b)]. The three methylene carbon atoms belonging to the independent malonate groups lie on a mirror plane. L1 adopts a $\mu_3-\kappa^2O:\kappa O':\kappa^2O'':\kappa O'''$ coordination mode forming two four- and one six-membered fused chelate rings with values of the angles subtended at the Ho(1)/Ho(1b) and Ho(2) of 48.56(13) and 72.7(2)°, respectively (Fig. 4a). L2 shows a $\mu_3-\kappa O:\kappa^2O':O'':\kappa O'''$ coordination mode exhibiting simultaneously bis-monodentate [through O(12) and O(12a) towards Ho(2) and Ho(2a), respectively] and bidentate [through O(11) and O(11a) towards Ho(2)] binding modes (Fig. 4b). Finally, L3 acts as a

bidentate ligand through the O(21) and O(21b) atoms towards Ho(2) [O(21)-Ho(2)-O(21b) = 75.6(3)°] (Fig. 4c).

Each triaquaholmium(III) unit is connected to four

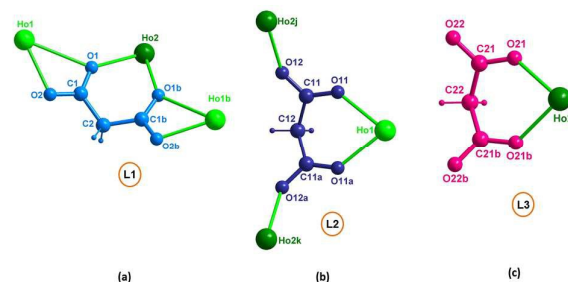


Fig. 4. Coordination modes of the crystallographically independent malonate ligands in **1·2H₂O**.

diaquaholmium(III) entities by four carboxylate groups from three different malonate ligands to form corrugated layers (see Fig. 1). The shortest values of the intralayer separation between the holmium centres are 4.9314(5) [Ho(1)⋯Ho(2) through L1], 5.9648(6) [Ho(1)⋯Ho(2j) across L2], 8.0555(9) [Ho(1)⋯Ho(1b) and Ho(2j)⋯Ho(2k) through L1 and L2, respectively], 7.0905(8) [Ho(1)⋯Ho(1k)] and 6.384(8) Å [Ho(2)⋯Ho(2j)] (Fig. 1a). The corrugated layers of the holmium(III) ions are stacked in an *ABAB* sequence being and interlinked by hydrogen bonds involving water molecules and malonate-oxygen atoms to build a supramolecular three-dimensional network (Fig. 2). The distance between adjacent mean planes defined by the holmium(III) ions is 10.104(3) Å.

[Ce₂(mal)₃(H₂O)₆]₂·2(H₂O) (**3·2H₂O**). The structure of **3·2H₂O** is similar to the previously reported structure for [Sm₂(mal)₃(H₂O)₆] (**2**).^{7f} Their structures consist of three-dimensional malonate-bridged triaqualanthanide(III) networks [Figs. 5a (**2**) and 5b (**3·2H₂O**)] which result from the cross-linking of chains of lanthanide pairs [Ln = Sm(III) (**2**) and Ce(III) (**3·2H₂O**)] which grow along the [101] direction [Figs. 6b (**2**) and 7b (**3·2H₂O**)] and other chains running parallel to the crystallographic *c*-axis [Figs. 6a (**2**) and 7a (**3**)]. Each lanthanide(III) ion in this three-dimensional network is connected to seven metal centres through four malonate ligands giving rise to a moganite type binodal network [(4⁶ 4⁸)₂(4² 6² 8²)-mog in Schläfli notation]. Extensive hydrogen bonding involving coordinated (**2**) and non-coordinated water molecules (**3**) contribute to stabilize the supramolecular three-dimensional networks of the complexes **2** and **3** [Tables S2 (**2**) and S3. ESI† (**3·2H₂O**)].

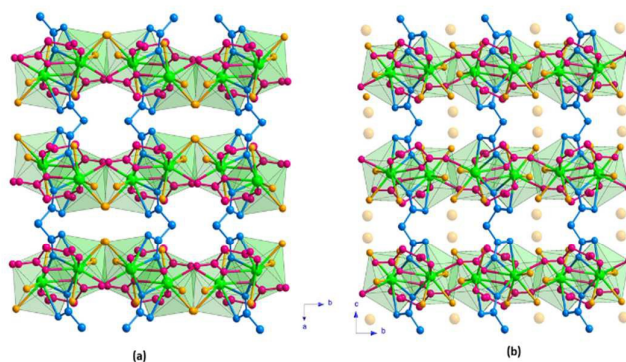


Fig. 5. Perspective view of the crystal packing in **2** (a) and **3·2H₂O** (b). Pink and blue colours denoted the crystallographically different malonate ligands that occur in both compounds. Hydrogen bonds were not drawn for clarity.

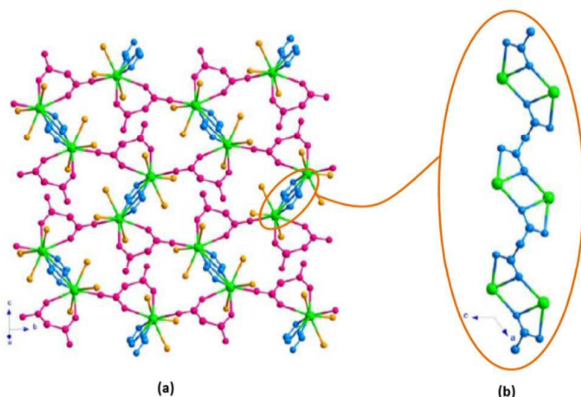


Fig. 6. Perspective views of (a) the chains that run parallel to the crystallographic *c*-axis and (b) the chain of pairs of Sm(III) ions that grow along the [101] direction in compound **2**.

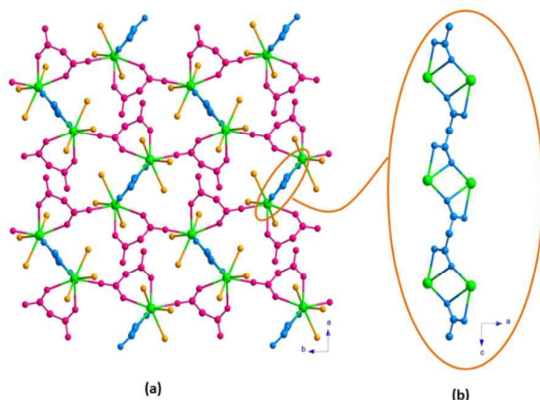


Fig. 7. Perspective views of (a) the chains that run parallel to the crystallographic *c*-axis and (b) the chain of pairs of Ce(III) ions that grow along the [101] direction in **3·2H₂O**.

The Sm(III) (**2**) and Ce(III) (**3·2H₂O**) ions are nine-coordinate (**Fig. 8**). Six carboxylate oxygen atoms from three different malonate groups [values of the Ln-O(mal) bond distances in the ranges 2.321(5)-2.602(4) Å (**2**) and 2.436(4)-2.729(3) Å in (**3**)] and three water molecules [Ln-O(w) = 2.484(4)-2.532(4) Å (**2**) and 2.507(4)-2.557(4) Å (**3·2H₂O**)] build distorted monocapped square antiprisms around the two rare earth atoms.

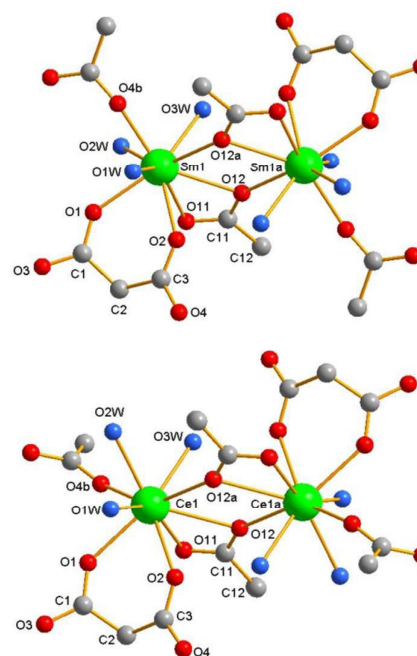


Fig. 8. A view of the Sm(III) (top) and Ce(III) (bottom) environments in compounds **2** and **3·2H₂O** respectively, showing the atom numbering [symmetry code: (a) = $-x+1/2, -y+1/2, -z$ and (b) = $-x+1/2, y+1/2, -z+1/2$ for **2** and (a) = $-x, -y, -z-1$ and (b) = $-x+1/2, +y-1/2, z$ for **3·2H₂O**].

Two crystallographically independent malonate groups, L1 [C(1)-C(2)-C(3) (**2**) and (**3·2H₂O**)] and L2 [C(11)-C(12)-C(11i) (**2**) and C(11)-C(12)-C(11g) (**3·2H₂O**)] are present in these two compounds (**Fig. 9**). L1 exhibits the $\mu\text{-}\kappa^2\text{O}':\kappa^2\text{O}'':\text{O}''$ binding mode, adopting simultaneously monodentate [through O(4) towards Sm(1g) and Ce(1f)] and bidentate [through O(1) and O(2) towards Sm(1) and Ce(1)] coordination modes, the value of the angle subtended by the malonate ligand at the lanthanide atom being 71.54(12) (**2**) and 69.59(11)° (**3·2H₂O**). The carboxylate(malonate) bridge [O(4)C(3)O(2)] adopts the *anti-syn* conformation.

The methylene-carbon atom [C(12)] from L2 lies on a two-fold axis. This malonate group links four lanthanide atoms ($\mu_4\text{-}\kappa^2\text{O}':\kappa\text{O}'':\kappa^2\text{O}'':\kappa\text{O}'''$) acting simultaneously as bis-monodentate [through O(12) and O(12i) towards Sm(1h) and Sm(1j)] and across O(12) and O(12g) towards Ce(1a) and Ce(1h)] and bis-bidentate ligand [across the carboxylate-malonate oxygen atoms towards the lanthanide(III) ions], the value of the angle subtended by carboxylate(malonate) group at the rare earth atoms being 50.16(11)° (**2**) and 48.47(11)° (**3·2H₂O**). The structural parameters of L1 and L2 agree with those reported for other malonate complexes.

Each triquanthanide(III) units are linked by the malonate skeleton of the L1 group leading to a chain of lanthanide(III) ions growing along the crystallographic *b*-axis. The shortest values of the intrachain Ln...Ln distance are 6.5858(10) and 6.7313(7) Å for **2** and **3**, respectively.

These malonate-bridged lanthanide chains are further linked through the carboxylate-malonate unit of the L2 group, the distance through the double μ -oxo(carboxylate) bridge being 4.2971(7) (**2**) and 4.4656(4) Å (**3**·**2H₂O**). A 3D structure through the pillaring role of the L2 ligand results in **2** (Figs. **9a** and **9b**). The shortest values of the interlayer Ln^{III}Ln distance are 6.971(2) Å (**2**) and 7.9207 Å (**3**·**2H₂O**) and the stacking of these layers follows the ABABA (**2**) and AAAAA (**3**) trends.

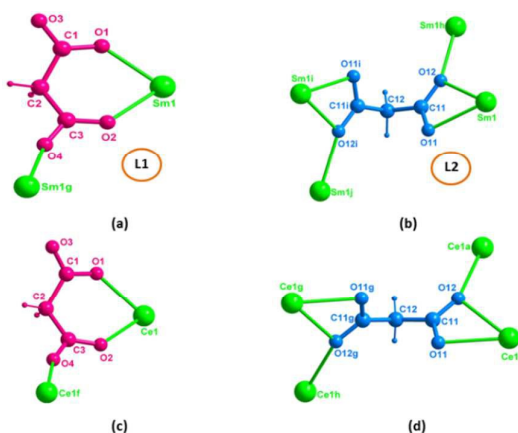


Fig. 9. Coordination modes of the two crystallographically independent malonate ligands in **2** ((a) and (b)) and in **3**·**2H₂O** ((c) and (d)).

[Ce₂(mal)₃(H₂O)₃]**2H₂O** (**4**·**2H₂O**). The structure of **4**·**2H₂O** can be described as chains of cerium(III) ions linked through two crystallographically independent malonate ligands (L1 and L2) which run parallel to the crystallographic *a* axis (Fig. **10a**) that in turn are linked along the crystallographic *b* axis through a new independent malonate ligand (L3) resulting in a neutral two-dimensional structure (Fig. **11b**). A weak hydrogen bond between one coordinated water molecule [O(2w)] and a carboxylate-oxygen atom [O(5)], [O(2w)⋯O(5b)] = 3.0796(4) Å occurs within each layer. The two-dimensional network of **4** can be found in different malonate complexes with other trivalent lanthanide ions.⁷ Further stabilization of the crystal structure is achieved by an extensive hydrogen bonding involving carboxylate groups and water molecules, leading to a supramolecular three-dimensional network (Table S4, ESI†).

Two of the three crystallographically independent malonate groups (L1 and L2 in Figs. **11a** and **11b**, respectively) exhibit identical μ_3 - κ^2 O: κ O': κ^2 O'': κ O''' binding mode, the six-membered rings having the boat conformation. The values of the cerium-cerium separation through the carboxylate-oxygen bridges are 4.4621(4) [Ce(1)⋯Ce(2) across O(1) and O(12)] and 4.2301(10) Å [Ce(1)⋯Ce(2b) and Ce(1a)⋯Ce(2) through O(3) and O(9), respectively; symmetry code: (a) = -1+x, y, z and (b) = 1+x, y, z]. L3 exhibits the μ_3 - κ O: κ^2 O': κ^2 O'': κ O''' binding mode adopting simultaneously bidentate [at Ce(2c); symmetry code: (c) = -x, -0.5+x, 2-z] and monodentate [at Ce(1) and Ce(2)] coordination modes. The six-membered ring formed by the chelation of Ce(2c) through O(6) and O(8) exhibits also a boat conformation. L3 connects the cerium ions through two carboxylate bridges [O(5)C(4)O(6) and O(7)C(6)O(8)] exhibiting the *anti-anti* conformation, the values of the Ce(2c)⋯Ce(1) and Ce(2c)⋯Ce(2) separations through them being 6.9600(9)

and 6.7823(8) Å, respectively (Fig. **11c**). The average C-O bond distances and O-C-O bond angles are 1.265(8) Å and 120.4(6)° for L1 and L2, and 1.269(8) Å and 122.1(6)° for L3. These values are in agreement with those of the previously reported

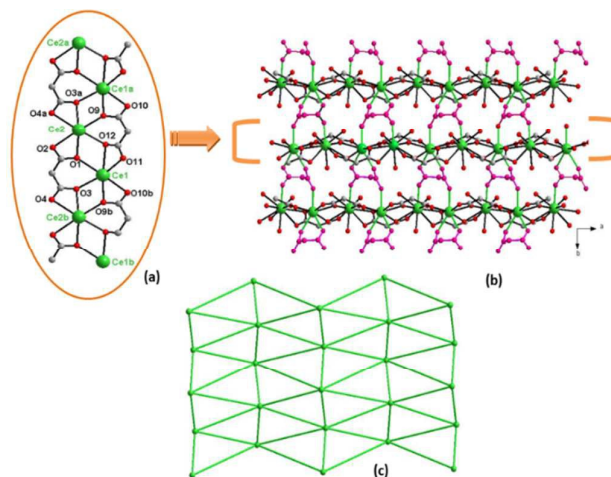


Fig. 10. Perspective views of (a) the chain and (b) a fragment of the layer and (c) a schematic view along the crystallographic *c*-axis in the (110) plane of **4**·**2H₂O**.

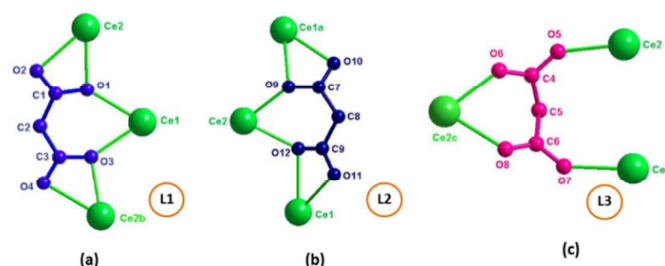


Fig. 11. Coordination modes of the three crystallographically independent malonate ligands that occur in **4**·**2H₂O**.

malonate-containing lanthanide(III) complexes.⁷

The two crystallographically independent cerium(III) ions are ten- [Ce(1)] and nine- [Ce(2)] coordinate in distorted bi-capped dodecahedron [Ce(1)] and monocapped square antiprism [Ce(2)] surroundings. Ce(1) is coordinated by three water molecules and five malonate ligands, while the nine oxygen atoms bound to Ce(2) come from five different malonate groups (Fig. **12**). The Ce(1)-O bond distances are in the range 2.453(4)-2.741(5) Å, their mean value being 2.585(5) Å. The Ce(2)-O bond distances are smaller and they lie in the range 2.391(5)-2.695(5) Å, with an average value of 2.530(5) Å. Both geometries are observed in other lanthanide(III)-malonate complexes reported in the literature.⁷ Regular alternating of the Ce(1) and Ce(2) atoms occurs within the chain along the crystallographic *a* axis with sharing of the O(3)-O(9b) edge (Fig. **10a**). The values of the shortest interchain Ce⋯Ce separation through the *anti-anti* carboxylate bridge [6.9600(9) and 6.7823(8) Å] are shorter than the shortest interlayer one.

On heating, the onset of the endothermic change occurs at $-18\text{ }^{\circ}\text{C}$ and it reaches a maximum at about $-16\text{ }^{\circ}\text{C}$. On cooling, the onset of the peak is shifted to somewhat lower temperatures (about $-27\text{ }^{\circ}\text{C}$) and the minimum peak is found at $-29\text{ }^{\circ}\text{C}$. These differences during the heating and cooling processes can be attributed to hysteresis phenomena. The phase transformation can be considered of first-order type due to thermal hysteresis observed (around $9\text{ }^{\circ}\text{C}$).

The enthalpy change at the phase transition ($\Delta H \sim 764,1\text{ J mol}^{-1}$) was calculated by numerical integration of the recorded DSC curves, after the correction for the calorimetric base line, using the relationship $\Delta H = \int Q/\beta dt$, where Q , β and t are the heat flow, heating rate and time, respectively.²³ A similar phase transition was also observed in other lanthanide(III)-malonate complexes ($[\text{Ln}_2(\text{mal})_3(\text{H}_2\text{O})_6]$ with $\text{Ln} = \text{Eu}$ or Gd) previously studied by our research group.^{7i,7m} However, these complexes showed lower values of the enthalpy change and an absence of thermal hysteresis, indicating predominant second order phase transitions. These results suggest a change in the phase transition from the first order for cerium-complex to nearly second order for the Eu/Gd derivatives, reflecting the decrease in the ionic radius along the f-block series.

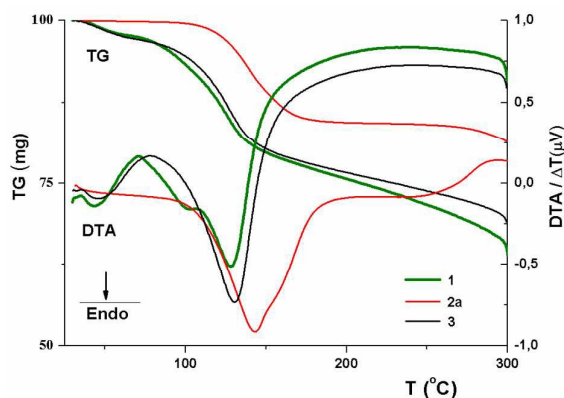


Fig. 14. TG/DTA curves of $1\cdot 2\text{H}_2\text{O}$ (green), 2a (red) and $3\cdot 2\text{H}_2\text{O}$ (black). TG = mass loss (mg); DTA = ΔT (μV) and (\downarrow endo)

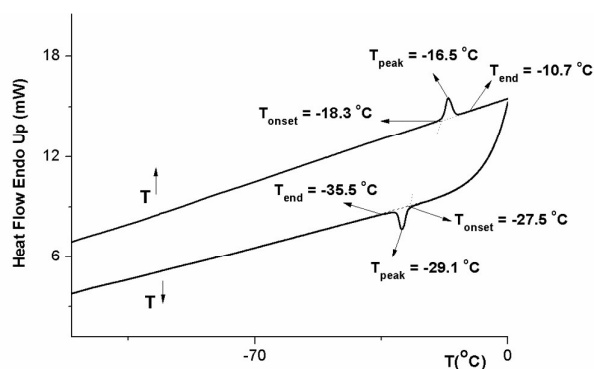


Fig. 15 DSC curves of 2a for increasing and lowering temperatures.

3.4 Preparative routes and structural remarks on malonate-based lanthanide(III) CPs

The malonate ligand has been used to synthesize several lanthanide containing compounds (Table 3), and their thermogravimetric behaviour and photoluminescent and magnetic properties have been investigated. Although it is difficult to predict their crystal structures, these compounds contribute to the studies about the behaviour of the lanthanide complexes, as well as to their structural patterns.

a) Synthetic routes

The more traditional and commonly used crystal growth methods are the solvent evaporation or cooling a saturated solution and the hydro(solvo)thermal methods (see ESI[†]), the latter one used only to obtain the $[\text{Dy}_2(\text{mal})_3(\text{H}_2\text{O})_6]$ complex.^{7h}

On the other hand, a variety of other methods combining known metal coordination environments with multifunctional exdentate ligands had led to the preparation of a wide variety of crystalline architectures.

Taking into account the above consideration, we have prepared new complexes under slow diffusion of aqueous solutions of lanthanide(III)-nitrates into a gel of sodium metasilicate containing malonic acid (H_2mal). The principle of this method is to slowly bring the different species into contact. One approach is the solvent liquid diffusion where first of all, two layers with different densities are formed: one contains the product in a solvent and the other one is the precipitant solvent, a solvent layer separating each other. The precipitant solvent slowly diffuses into the separate layer and the crystal growth occurs at the interface. The other approach is the slow diffusion of reactants by the separation of physical barriers, such as two vials with different size. Additionally, gels are also used as diffusion and crystallization media in some cases, in particular to slow down the diffusion process and to avoid precipitation of the bulk material. The diffusion method is preferred to grow X-ray quality crystals instead of polycrystalline or poorly diffracting powdered products, especially if the products have a low solubility.

b) Inorganic skeleton

Also, this work reveals the great diversity of lanthanide MOFs obtained by the use of the malonate ligand in contrast to the lanthanide(III)-oxide architectures: the flexibility and variety of the coordination modes of the malonate group compared to the rigidity and more limited bonding modes of the oxo ligand account for this great diversity of the malonate-containing lanthanide complexes.

One of the reasons for the richness of these systems relates to the high values of the coordination number and characteristic geometries of the Ln(III) ions. This is despite the limited number of secondary building units (SBUs) in Ln(III)-based systems compared to CPs based on M(II). Considering the inorganic framework in the crystal structures, one can see dinuclear moieties with polyhedral sharing edges as well as their aggregation into chains and layers (Fig. 16). This diversity implies a great number of connecting possibilities with the organic moieties, which are also numerous as shown in this work. It is well known that the trivalent lanthanide cations undergo hydrolysis reactions in aqueous very easily (because of their high charge and small size) leading to polynuclear species and both the pH and temperature of the solutions have a strong influence on the nuclearity degree of the polynuclear

Journal Name

ARTICLE

species, the synthetic conditions being then crucial to determine the degree of condensation of the oligonuclear units.^{24,25}

CrystEngComm Accepted Manuscript

Table 3. List of malonate-based lanthanide(III) coordination polymers

Compound	Coordination Geometry	Ln-O (Å)	n _{H₂O}	D	Synthesis	Space Group	CSD	Ref.
[Ln ₂ (mal) ₃ (H ₂ O) ₆] _n	9(6-O _c , 3-O _w)							
Phase I^{room temperature}								
Nd	DMSA	2.400(1)-2.565(8)	6	3D	G at 293 K	C2/c	AQMAND01	7i
Eu	DMSA	2.303(4)-2.596(3)	6	3D	H at 363 K	C2/c	XUBJAF02	7n
Eu	DMSA	2.307(4)-2.605(4)	6	3D	SE at 293 K	C2/c	XUBJAF03	7s
Dy	DTTP	2.326(3)-2.610(2)	6	--	H at 433 K	C2/c	YOCMAF	7o
Pr	DMSA	2.366(3)-2.634(3)	6	3D	G at 293 K	C2/c	ALALUU	7j
Sm	DMSA	2.319(5)-2.611(4)	6	3D	H at 363 K	C2/c	LEPLEZ	7s
Gd	--	--	6	--	--	C2/c	AKUHOD01	7t
Sm	DMSA	2.321(6)-2.602(4)	6	3D	G at 293 K	C2/c	--	this work
Ce;Pr;Nd;Sm (XRPD)	--	--	6	--	--	C2/c	--	this work
Phase II^{room temperature}								
Pr	DCTA	--	6	3D	SE at 298 K	I2/a	ALALUU01	7r
Nd	DMSA-DTTP	2.50 (medium)	6	3D	SE at 295 K	I2/a or Ia	AQMAND	7b
Eu	DMSA	2.310(5)-2.532(5)	6	3D	G at 293 K	I2/a	XUBJAF01	7i
Gd	DMSA	2.308(2)-2.597(2)	6	3D	G at 293 K	I2/a	AKUHOD	7k
Gd	DMSA	2.308(2)-2.587(2)	6	3D	G at 293 K	I2/a	AKUHOD02	7m
Phase II^{low temperature}								
Eu	DCA	2.287(4)-2.605(7)	6	3D	G at 173 K	Ia	XUBJAF	7i
Gd	CAP	2.273(5)-2.608(6)	6	3D	G at 173 K	Ia	AKUHOD03	7m
[Ln ₂ (mal) ₃ (H ₂ O) ₆] _n ·2nH ₂ O	9(6-O _c , 3-O _w)							
Nd	DMSA	2.41(1)-2.72(1)	8	3D	SE at 295 K	Pbcn	AMALND	7a
Pr	--	--	8	3D	SE at 298 K	Pnab	EPUJII	7r
Ce	DMSA	2.436(4)-2.729(3)	8	3	G at 303 K	Pbcn	--	this work
[Ln ₂ (mal) ₃ (H ₂ O) ₆] _n ·3nH ₂ O	9(6-O _c , 3-O _w); 8(6-O _c , 2-O _w)							
Eu	DTTP; DSA	2.37(2)-2.84(2)	8	2D	SE at 295 K	Pnma	AMALEU	7c
Gd	DMSA; DSA	2.344(7)-2.820(8)	7	2D	G at 293 K	Pmnb	VEWDIL	7m
Ho	DMSA; DSA	2.307(4)-2.843(4)	7	2D	G at 303 K	Pnma	--	this work
Gd;Eu;Tb;Dy;Ho;Er;Yb(XRPD)	DMSA; DSA	2.307(4)-2.843(4)	7	--	P at 293 K	Pnma	--	this work
[Ln ₂ (mal) ₃ (H ₂ O) ₄] _n ·nH ₂ O	10(8-O _c , 2-O _w)							
La		2.412(3)-2.688(2)	5	3D	SE at 295 K	C2/c	CEWNIB	7g
[Ln ₂ (mal) ₃ (H ₂ O) ₃] _n ·2nH ₂ O	9(6-O _c , 3-O _w); 10(8-O _c , 2-O _w)							
Pr	DMSA; DBD	2.394(5)-2.719(5)	5	2D	G at 295 K	P2 ₁	LOSWAR	7h
La			5	2D	SE at 295 K	P2 ₁ /n	POPKAG	7e
Ce	DMSA; DBD	2.394(5)-2.719(5)	5	2D	G at 303 K	P2 ₁	LOSWAR	this work
[Ln ₂ (Hmal)(mal)(H ₂ O) ₂] _n ·H ₂ O	10(8-O _c , 2-O _w)							
La	DTT		3	2D	SE at 295 K	P2 ₁ /n	YEGRUX	7f
[Ln(Hmal)(mal)]·4H ₂ O	9(6-O _c , 3-O _w)							
Sm	DMSA	2.453(6)-2.51(6)	4	3D	SE at 333 K	Pbnc		7w

Compound: XRPD = X-Ray Powder Diffraction; **Coordination Geometry:** O_c = carboxylate-oxygen; O_w = water-oxygen; DMSA = Distorted Monocapped Square-Antiprism; DTTP = Distorted Tricapped Trigonal Prism; DCTA = Distorted Capped Tetragonal Antiprism; DCA = Distorted Capped Antiprism; CSA = Monocapped Square Antiprism; DTTP = Distorted Tricapped Trigonal Prism; DSA = Distorted Square Antiprism; DBD = Distorted Bicapped Dodecahedron; DTT = Distorted Tetracapped Trigonal; **Dimensionality** = nD (n = 2, 3); **Synthesis:** G = Gel; H = Hydrothermal; SE = Slow Evaporation; P = Precipitation.

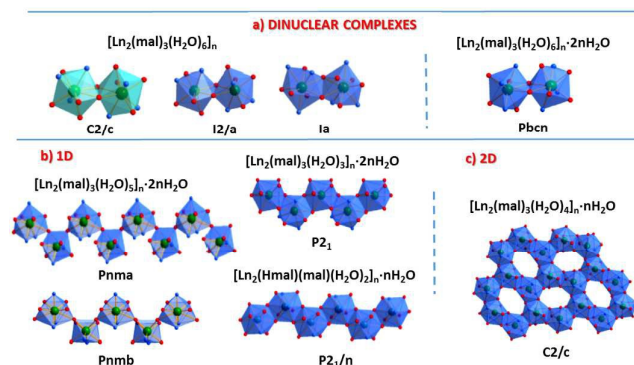


Fig. 16. Views of the oligonuclear units for the malonate-based complexes listed in Table 3.

In general, looking at the structure of the Ln(III)-malonate compounds, it can be seen that changes in the conditions of the gel synthesis lead to different phases, demonstrating that this type of synthetic route is appropriate to obtain different phases. Furthermore, a mixed-ligand complex of formula $\{Na[Gd(mal)(ox)(H_2O)]\}_n$ ($ox = oxalate$) was obtained using the malonic acid as the only ligand.^{7m} For such a compound, this reaction is most likely mediated by the silica gel medium. After the incorporation of the gadolinium(III) salt into the gel and once the reaction starts, the initial conditions (pH and concentration of the reactants) change due to uncontrolled variable parameters inside the gel (reaction speed, product formation, etc.). Although it seems that such a part of the reaction is out of control, this situation let us explore thoroughly multiple synthetic conditions in one experiment looking for stable complexes. Then, the synthetic conditions which allowed the formation of the new ligand from the starting reagents could be achieved in the gel. The preference of the lanthanide(III) ions for the nine-coordination deserves also to be outlined.

c) Coordination modes of the malonate

We have used the Cambridge Structural Database (CSD)²⁶ search ConQuest program to retrieve the cif files corresponding to the malonate-containing homometallic lanthanide(III) complexes in order to look for all the reported coordination modes of this ligand. We restrain the search to those structures with an *R*-factor less than 10% and we skipped the structures described in the present work (Table 3). Once we got the *cif*-files, we analyse the coordination of the malonate groups in each retrieved structure. To enhance this task, we used the Diamond program that allowed us to represent conveniently the coordination mode of the malonate groups for each compound. The seven different coordination modes that we found are depicted in Fig. 17. One can see therein that the oxygen atoms of the two carboxylate groups of the malonate ligand are always involved in its coordination to the lanthanide ions with a marked trend to adopt bridging modes. The six-membered chelate ring commonly observed in the malonate complexes with the first-row transition metal ions is present here in four of the seven coordination modes and the occurrence of the bis-chelation through the two carboxylate groups is also quite common in the lanthanide complexes with malonate (three cases in Fig. 17).

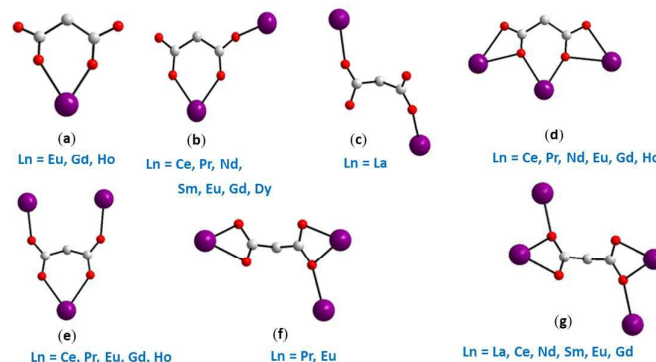


Fig. 17. Coordination modes of the malonate ligand in its homometallic lanthanide complexes: (a) κ^2O,O' ; (b) $\mu-\kappa O:\kappa^2O,O'$; (c) $\mu-\kappa O:\kappa O''$; (d) $\mu_3-\kappa^2O:\kappa O':\kappa^2O''':\kappa O''$; (e) $\mu_3-\kappa O:\kappa^2O,O':\kappa O''$; (f) $\mu_3-\kappa^2O,O':\kappa^2O''':\kappa O'''$ and (g) $\mu_4-\kappa^2O:\kappa O':\kappa^2O''$.

d) Topological analysis

A topological analysis among the 23 previously reported malonate-based lanthanide compounds shows the occurrence of nine families of compounds. Six of them present 2D and 3D arrangements being $(4^{12}6^3)$ -*pcu* α -Po primitive cubic,^{7b, 7i, 7k, 7m, 7r, 7t} $(4^64^8)_2(4^26^28^2)$ -*mog*,^{7a, 7j, 7l, 7m, 7r, 7s, 7u} 6^3 -*hcb* Shubnikov hexagonal plane,^{7c, 7m} $(4^46^2)(4^46^6)$ -*tcs*^{7b} and 3,3,3,4,5L5^{7h} networks (see Table 3).

4. Conclusions

In summary, we have successfully assembled malonate and Ln(III) salts into a series of 3D coordination frameworks, $[Ln_2(mal)_3(H_2O)_6]\cdot 2H_2O$ with Ln = Ho (1), Tb (1a), Dy (1b), Er (1c) and Yb (1d), $[Ln_2(mal)_3(H_2O)_6]$ with Ln = Sm (2), Ce (2a), $[Ce_2(mal)_3(H_2O)_6]\cdot 2H_2O$ (3) and $[Ce_2(mal)_3(H_2O)_3]\cdot 2H_2O$ (4). It was found that the synthetic conditions in the reaction process play a crucial role on the structural control of the complexes. The thermogravimetric analysis of 1-3 revealed the presence of thermal induced reversible phase transitions for compound 3 and also shows that different metal ions in the malonate complexes have important effects on the course of their thermal decomposition.

Acknowledgements

This work was supported by the MINECO (Projects MAT2014-57465-R, CTQ2013-44844P and Unidad de Excelencia Maria de Maetzu MDM-2015-0538), the Generalitat Valenciana (Projects PROMETEOII/2014/070 and ISIC/2012/002) and the Universitat de València (Project UV-INV-AE11-38904). C.R.-P. thanks a visiting Professorship of the Universitat de València (2015-2016) and J.P. thanks the MINECO for a postdoctoral grant.

References

- (a) S. R. Batten and R. Robson, *Angew. Chem., Int. Ed.*, 1998, **37**, 1460; (b) M. Fujita, Y. J. Kwon, S. Washizu and K. Ogura,

- J. Am. Chem. Soc.*, 1994, **116**, 1151; (c) G. B. Gardner, D. Venkataraman, J. S. Moore and S. Lee, *Nature* 1995, **374**, 792; (d) C. Piguat and J. C. G. Bünzli, *Chem. Soc. Rev.*, 1999, **28**, 347; (e) L. H. Gade, *Acc. Chem. Res.*, 2002, **35**, 575; (f) L. Carlucci, G. Ciani and D. M. Proserpio, *Coord. Chem. Rev.*, 2003, **246**, 247; (g) J. P. Zhang, S. L. Zheng, X. C. Huang and X. M. Chen, *Angew. Chem., Int. Ed.*, 2004, **43**, 206; (h) A. N. Khlobystov, A. J. Blake, N. R. Champness, D. A. Lemenovskii, A. G. Majouga, N. V. Zyk and M. Schröder, *Coord. Chem. Rev.*, 2001, **222**, 155; (i) O. M. Yaghi, M. O’Keeffe, N. W. Ockwig, H. K. Chae, M. Eddaoudi, and J. Kim, *Nature* 2003, **423**, 705; (j) B. Moulton and M. J. Zaworotko, *Chem. Rev.* 2001, **101**, 1629; (k) N. L. Rosi, J. Eckert, M. Eddaoudi, D. T. Vodak, J. Kim, M. O’Keeffe and O. M Yaghi, *Science* 2003, **300**, 1127; (l) S. Subramanian and M. J. Zaworotko, *Angew. Chem., Int. Ed.*, 1995, **34**, 2127; (m) S. Kitagawa, R. Kitaura and S. I. Noro, *Angew. Chem., Int. Ed.*, 2004, **43**, 2334; (n) D. Bradshaw, J. B. Claridge, E. J. Cussen, T. J. Prior and M. J. Rosseinsky, *Acc. Chem. Res.*, 2005, **38**, 273; (o) S. R. Batten, B. F. Hoskins and R. Robson, *Angew. Chem., Int. Ed.*, 1997, **36**, 636; (p) S. Hu, J. C. Chen, M. L. Tong, B. Wang, Y. X. Yan and S. R. Batten, *Angew. Chem., Int. Ed.*, 2005, **44**, 5471; (q) T. R. Cook, Y.-R. Zheng and P. J. Stang, *Chem. Rev.*, 2013, **113**, 734; (r) S. R. Batten, S. M. Neville, D. R. Turner, *Coordination Polymers. Design, Analysis and Application*, RSC Publishing, 2009.
- 2 (a) X. H. Bu, M. L. Tong, H. C. Chang, S. Kitagawa and S. R. Batten, *Angew. Chem., Int. Ed.*, 2004, **43**, 192; (b) O. R. Evans and W. Lin, *Acc. Chem. Res.*, 2002, **35**, 511; (c) G. Férey, C. Serre, C. Mellot-Draznieks, F. Millange, S. Surble, J. Dutour and I. Margiolaki, *Angew. Chem., Int. Ed.*, 2004, **43**, 6296; (d) P. J. Hagrman, D. Hagrman and J. Zubieta, *Angew. Chem., Int. Ed.*, 1999, **38**, 2638; (e) C. N. R. Rao, S. Natarajan and R. Vaidhyanathan, *Angew. Chem., Int. Ed.*, 2004, **43**, 466; (f) Y. B. Dong, M. D. Smith and H. C. zur Loye, *Angew. Chem., Int. Ed.*, 2000, **39**, 4271; (g) B. Zhao, P. Cheng, Y. Dai, C. Cheng, D. Z. Liao, S. P. Yan, Z. H. Jiang and G. L. Wang, *Angew. Chem., Int. Ed.*, 2003, **42**, 934; (h) B. Zhao, P. Cheng, X. Y. Chen, C. Cheng, W. Shi, D. Z. Liao, S. P. Yan, Z. H. Jiang, *J. Am. Chem. Soc.*, 2004, **126**, 3012; (i) R. Xiong, X. You, B. F. Abrahams, Z. Xue and C. Che, *Angew. Chem., Int. Ed.*, 2001, **40**, 4422; (j) R. J. Hill, D. L. Long, N. R. Champness, P. Hubberstey and M. Schröder, *Acc. Chem. Res.*, 2005, **38**, 337.
- 3 (a) N. L. Rosi, M. Eddaoudi, J. Kim, M. O’Keeffe and O. M. Yaghi, *Angew. Chem., Int. Ed.*, 2002, **114**, 294; (b) M. E. Braun, C. D. Steffek, J. Kim, P. G. Rasmussen and O. M. Yaghi, *Chem. Commun.*, 2001, 2532; (c) T. M. Reineke, M. Eddaoudi, M. Fehr, D. Kelley and O. M. Yaghi, *J. Am. Chem. Soc.*, 1999, **121**, 1651.
- 4 (a) T. M. Reineke, M. Eddaoudi, M. Fehr, D. Kelley and O. M. Yaghi, *J. Am. Chem. Soc.*, 1999, **121**, 1651; (b) A. Thirumurugan and S. Natarajan, *Dalton Trans.*, 2004, 2923; (c) D. L. Long, A. J. Blake, N. R. Champness, C. Wilson and M. Schröder, *Angew. Chem., Int. Ed.*, 2001, **40**, 2443; (d) Y. Wan, L. Jin, K. Wang, L. Zhang, X. Zheng, S. Lu, *New J. Chem.*, 2002, **26**, 1590; (e) B. D. Alleyne, A. R. Williams, L. A. Hall, *Inorg. Chem.*, 2001, **40**, 1045; (f) L. Pan, M. Zheng, Y. Wu, S. Han, R. Yang, X. Huang, J. Li, *Inorg. Chem.*, 2001, **40**, 828.
- 5 (a) O. Kahn, *Acc. Chem. Res.*, 2000, **33**, 647; (b) W. S. Liu, T. Q. Jiao, Y. Z. Li, Q. Z. Liu, M. Y. Tan, H. Wang and L. F. Wang, *J. Am. Chem. Soc.*, 2004, **126**, 2280; (c) B. Q. Ma, D. S. Zhang, S. Gao, T. Z. Jin, C. H. Yan and G. X. Xu, *Angew. Chem., Int. Ed.* 2002, **39**, 3644.; (d) C. Serre, N. Stock, T. Bein, G. Férey, *Inorg. Chem.*, 2004, **43**, 3159; (e) G. Mancino, A. J. Ferguson, A. Beeby, N. J. Long and T. S. Jones, *J. Am. Chem. Soc.*, 2005, **127**, 524.
- 6 (a) Y. J. Kim, M. Suh and D. Y. Jung, *Inorg. Chem.*, 2004, **43**, 245; (b) H. F. Zhu, Z. H. Zhang, T. A. Okamura, W. Y. Sun and N. Ueyama, *Cryst. Growth & Design.*, 2005, **5**, 177.
- 7 **Homometallic Ln(III)-malonate complexes.** (a) E. Hansson *Acta Chem. Scand.*, 1973, **27**, 2441; (b) E. Hansson, *Acta Chem. Scand.*, 1973, **27**, 2813; (c) E. Hansson, *Acta Chem. Scand.*, 1973, **27**, 2827; (d) E. Hansson, *Acta Chem. Scand.*, 1973, **27**, 2841; (e) F. Marrot and J.-C. Trombe, *C. R. Sciences Acad. Sci., Ser. II*, 1993, **317**, 319; (f) F. Marrot and J.-C. Trombe, *Polyhedron* 1994, **13**, 1931; (g) B. Benmerad, A. Guehria-Laidoudi, G. Bernardelli, F. Balegrone, *Acta Crystallogr.*, 2000, **C56**, 321; (h) M. Hernández-Molina, P. A. Lorenzo-Luis, T. López, C. Ruiz-Pérez, F. Lloret and M. Julve, *CrystEngComm.*, 2000, **2**, 169; (i) M. Hernández-Molina, P. Lorenzo-Luis, C. Ruiz-Pérez, T. López, I. R. Martín, K. M. Anderson, G. Orpen, E. H. Bocanegra F. Lloret and M. Julve, *Dalton Trans.*, 2002, 3462; (j) B. H. Doreswamy, M. Mahendra, M. A. Sridhar, J. S. Prasad, P. A. Varughese, K. V. Saban and G. Varghese, *J. Mol. Struct.*, 2003, **659**, 81; (k) M. Hernández-Molina, C. Ruiz-Pérez, F. Lloret and M. Julve, *Inorg. Chem.*, 2003, **42**, 5456; (l) B. H. Doreswamy, M. Mahendra, M. A. Sridhar, J. S. Prasad, P. A. Varughese, J. George and G. Varghese, *J. Materials Lett.*, 2005, **59**, 1206; (m) L. Cañadillas-Delgado, J. Pasán, O. Fabelo, M. Hernández-Molina, F. Lloret, M. Julve and C. Ruiz-Pérez, *Inorg. Chem.*, 2006, **45**, 10585; (n) Ch.-Z. Zhang, H.-Y. Mao, Y.-L. Wang, H.-Y. Zhang and J.-C. Tao, *J. Phys. Chem. Solid.*, 2007, **68**, 236; (o) Z.-Q. Fang, R.-H. Zeng, Z.-F. Song and M. Yang, *Acta Crystallogr.*, 2008, **E64**, m877; (p) M.-L. Guo and C.-H. Guo, *Acta Crystallogr.*, 2009, **C65**, m195; (q) R. Koner and I. Goldberg, *Acta Crystallogr.*, 2009, **C65**, m160; (r) K. E. Chrysomallidou, S. P. Perlepes, A. Terzis, C.P. Raptopoulou, *Polyhedron* 2010, **29**, 3118; (s) J. Jin, X. Wang, Y. Li, Y. Chi and S. Niu, *Struct. Chem.*, 2012, **23**, 1523; (t) M.R.J. Elsegood and S. Husain, *Private Communication*, 2014; (u) I.A. Charushnikova, N.N. Krot and I.N. Polyakova, *Private Communication*, 2005; (v) P. Silva, J.A. Fernandes and F.A.A. Paz, *Acta Crystallogr.*, 2010, **E66**, m1514; (w) X. Wenmei, W. Qiguang, Y. Lan and Y. Ruding, *Polyhedron*, 1992, **11**, 2051.
- 8 Z.-M. Wang, L. J. van de Burgt and G., R. Choppin, *Inorg. Chimica Acta* 2000, **310**, 248.
- 9 (a) M. Insausti, R. Cortés, M. I. Arriortua, T. Rojo and, E. H. Bocanegra, *Solid State Ionics*, 1993, **63**, 351; (b) I. Gil de Muro, F. A. Mautner, M. Insausti, L. Lezama, M. I. Arriortua and T. Rojo, *Inorg. Chem.*, 1998, **37**, 3243; (c) I. Gil de Muro, M. Insausti, L. Lezama, J. L. Pizarro, M. I. Arriortua and T. Rojo, *Eur. J. Inorg. Chem.*, 1999, 935.
- 10 (a) A.P. Milanov, R.W. Seidel, D. Barreca, A. Gasparotto, M. Winter, J. Feydt, S. Irsen, H.-W. Becker and A. Devi, *Dalton Trans.*, 2011, **40**, 62; (b) A. Devi, *Coord. Chem. Rev.*, 2013, **257**, 3332.
- 11 H.K. Henisch, *Crystal Growth in Gels*, The Pennsylvania State University Press, University Park, London, 1970.
- 12 R.W.W. Hooft, *COLLECT*. Nonius BV, Delft, The Netherlands, 1999.
- 13 EVALCCD, A.J.M. Duisenberg, L.M.J. Kroon-Batenburg and A.M.M. Schreurs, *J. Appl. Cryst.*, 2003, **36**, 220.
- 14 SADABS version 2.03. Bruker AXS Inc.: Madison, WI, 2000.
- 15 L. J. Farrugia, *J. Appl. Cryst.*, 2012, **45**, 849.
- 16 G. M. Sheldrick, *Acta Crystallogr.*, 2008, **A64**, 112.
- 17 PARST97 Nardelli M. *J. Appl. Crystallogr.*, 1995, **28**, 659.

Journal Name

ARTICLE

- 18 DIAMOND 2.1d, *Crystal Impact* GbR., CRYSTAL IMPACT, K. Brandenburg & H. Putz GbR, Postfach 1251, D-53002 Bonn, Germany, 2000.
- 19 H. M. Rietveld, *J. Appl. Crystallogr.*, 1969, 2, 65.
- 20 J. Rodríguez-Carvajal, *Phys. Rev.*, B 1992, 192, 55. The programs of the FullProf Suite and their documentation can be obtained from Web at <http://www.ill.eu/sites/fullprof/>.
- 21 D. Cremer and J. A. Pople, *J. Am. Chem. Soc.*, 1975, 97, 1354.
- 22 K. Muraishi, Y. Suzuki and Y. Takanashi, *Thermochim. Acta* 1996, 286, 187.
- 23 J. L. McNaughton and C.T.Mortimer, *Differential Scanning Calorimetry*, Perkin Elmer, Order No. L-604 (reprinted from IRS, *Phys. Chem. Ser.*, Vol. 10, 1-44, Butterworths, London, 1975.
- 24 C. F. Baes, Jr., R. E. Mesmer. *The Hydrolysis of Cations*; John Wiley & Sons: New York, 1976; Chapter 7, pp 138–146.
- 25 A. Ikeda-Ohno, S. Tsushima, C. Hennig, T. Yaita, G. Bernhard, *Dalton Trans.* 2012, 41, 7190.
- 26 The Cambridge Structural Database. (a) C. R. Groom, I. J. Bruno, M. P. Lightfoot and S. C. Ward, *Acta Crystallogr.* 2016, B72, 171; (b) F. H. Allen, *Acta Crystallogr.* 2002, B58, 380.

Crystal growth and structural remarks in malonate-based lanthanide coordination polymers

Fernando S. Delgado, Pablo Lorenzo-Luís, Jorge Pasán, Laura Cañadillas-Delgado, Oscar Fabelo, María Hernández-Molina, Antonio D. Lozano-Gorrín, Francesc Lloret, Miguel Julve and Catalina Ruiz-Pérez*

*Corresponding author. E-mail: caruiz@ull.ull.es

Graphical abstract

The synthesis, structural characterization and thermal investigation of several malonate-containing lanthanide(III) complexes are provided herein together with a detailed structural overview of the twenty-three previously reported homometallic Ln(III)-malonate systems.

